

# DVCS off the Neutron in Jlab Hall A (6 GeV experiments)

Meriem BENALI

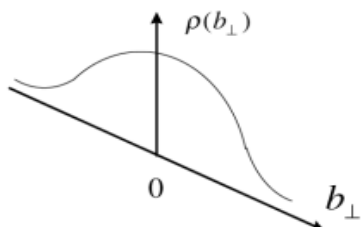
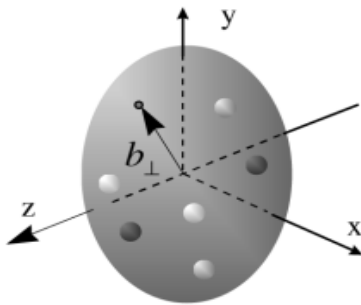


*Faculte des Sciences de Monastir (Tunisia)*



# Generalized Parton Distribution GPDs

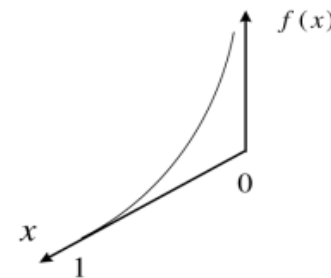
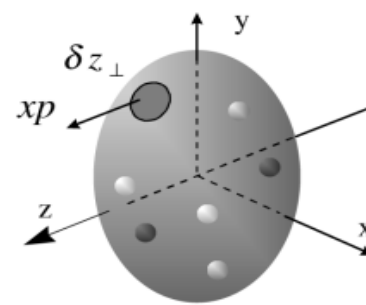
Elastic Scattering



## Form Factors

(Transverse position of partons)

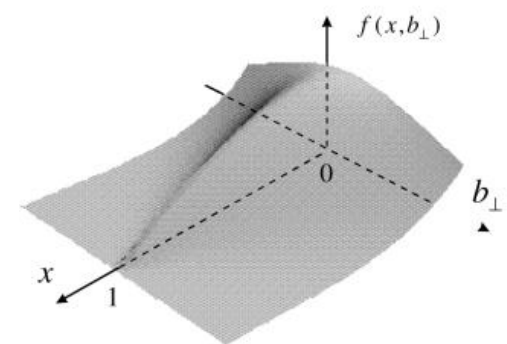
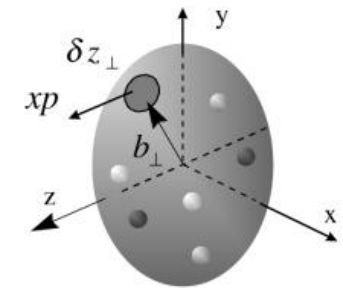
Deep inelastic scattering



## Parton Distribution Function ( PDFs)

(Longitudinal momentum distribution  
of the partons in the nucleon)

Deep exclusive scattering



## Generalized Parton Distribution GPDs

Two independent informations  
about the nucleon structure

**Correlate**

**3-D picture of the nucleon**

# Generalized Parton Distribution GPDs

At leading order, 8 GPDs for each flavor quark  $f$ :

- 4 chiral even GPDs :

$$H^f(x, \xi, t), E^f(x, \xi, t), \tilde{H}^f(x, \xi, t), \tilde{E}^f(x, \xi, t) \quad \text{Conserve the parton helicity}$$

- 4 chiral odd (transversity) GPDs:

$$H_T^f(x, \xi, t), E_T^f(x, \xi, t), \tilde{H}_T^f(x, \xi, t), \tilde{E}_T^f(x, \xi, t) \quad \text{Flip the parton helicity}$$

➤ Link to Parton distribution functions  
at ( $\xi=t=0$ )

$$\begin{aligned} H^q(x, 0, 0) & \left\{ \begin{array}{ll} = q(x); & x > 0 \\ = -\bar{q}(x) & x < 0 \end{array} \right. \\ \tilde{H}^q(x, 0, 0) & \left\{ \begin{array}{ll} = \Delta q(x); & x > 0 \\ = \Delta \bar{q}(-x); & x < 0 \end{array} \right. \\ \tilde{H}_T^q(x, 0, 0) & \left\{ \begin{array}{ll} = \delta q(x); & x > 0 \\ = \delta \bar{q}(-x); & x < 0 \end{array} \right. \end{aligned}$$

➤ Link to Form Factors ( $\forall \xi$ )

$$\begin{aligned} \sum_q e_q \int_{-1}^1 dx H^q(x, \xi, t) &= F_1(t) \\ \sum_q e_q \int_{-1}^1 dx E^q(x, \xi, t) &= F_2(t) \\ \sum_q e_q \int_{-1}^1 dx \tilde{H}^q(x, \xi, t) &= G_A(t) \\ \sum_q e_q \int_{-1}^1 dx \tilde{H}^q(x, \xi, t) &= G_p(t) \\ \sum_q e_q \int_{-1}^1 dx \tilde{H}_T^q(x, \xi, t) &= G_T(t) \end{aligned}$$

# Generalized Parton Distribution GPDs

At leading order, 8 GPDs for each flavor quark  $f$ :

- 4 chiral even GPDs :

$$H^f(x, \xi, t), E^f(x, \xi, t), \tilde{H}^f(x, \xi, t), \tilde{E}^f(x, \xi, t) \quad \text{Conserve the parton helicity}$$

- 4 chiral odd (transversity) GPDs:

$$H_t^f(x, \xi, t), E_t^f(x, \xi, t), \tilde{H}_t^f(x, \xi, t), \tilde{E}_t^f(x, \xi, t) \quad \text{Flip the parton helicity}$$

➤ Access to **quark angular momentum**, via **Ji sum rule [X. Ji 1997]**:

$$\frac{1}{2} \int_{-1}^{+1} dx x [H_q(x, \xi, t=0) + E_q(x, \xi, t=0)] = \boxed{J_q} = \frac{1}{2} \Delta \Sigma_q + L_q$$

➤ Solving the problem of the "spin puzzle"

$$\frac{1}{2} = \boxed{\frac{1}{2} \Delta \Sigma_q + L_q} + J_g$$

quark spin contribution ( $\sim 30\%$  of total spin)       $J_q$       quark orbital angular momentum      ???

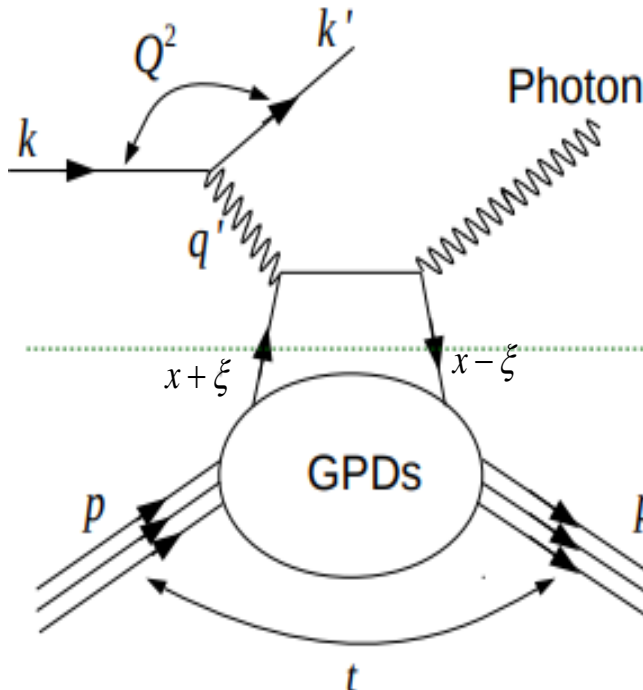
# How to access GPDs ?

The **deep exclusive processes** in the Bjorken regime are the simplest process which can be described in terms of GPDs by measuring its cross section

$$\begin{cases} Q^2 = -(k - k')^2 \rightarrow \infty \\ \nu = (k_0 - k'_0) \rightarrow \infty \end{cases}$$

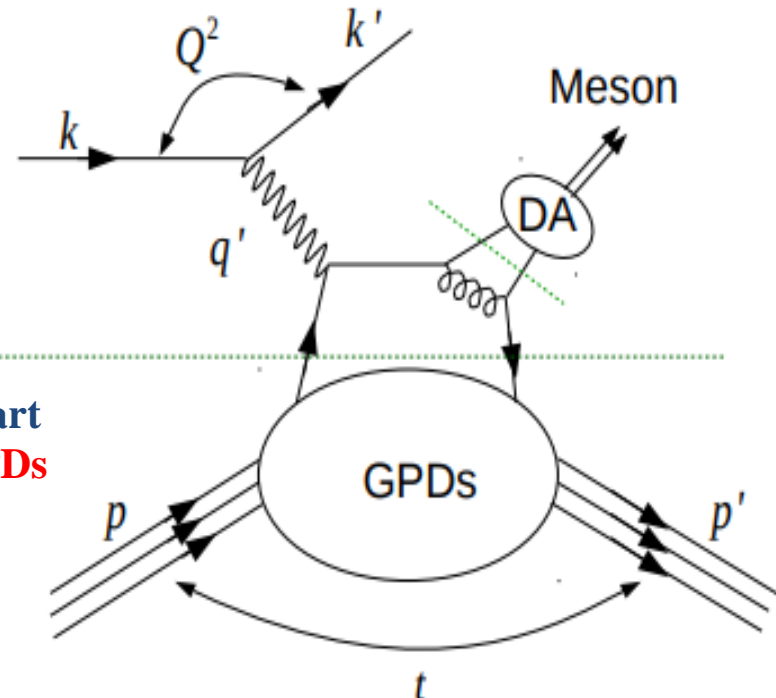
and fixed

$$x_B = \frac{Q^2}{2M\nu}$$



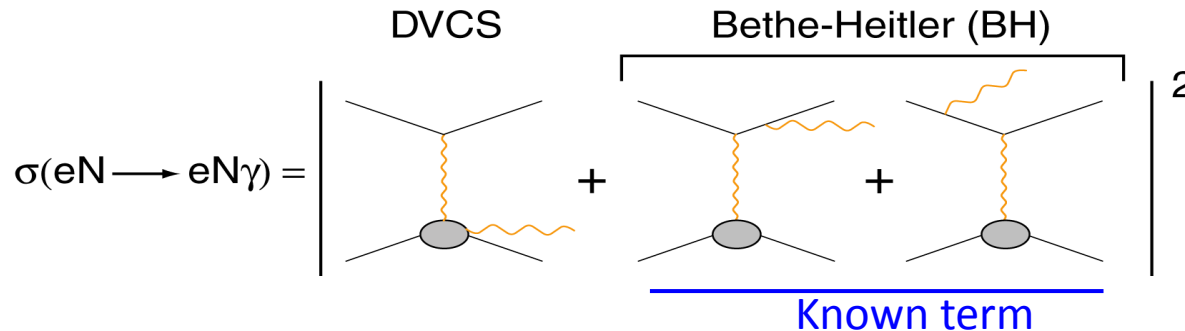
Deeply Virtual Compton Scattering  
(DVCS)

Perturbative part  
(calculable)



Deeply Virtual Meson Production  
(DVMP)

# Deeply Virtual Compton Scattering



The **unpolarized cross section** accesses the **real** part of the **interference** and the  $|T^{DVCS}|^2$  term which are sensitive to an **integral of GPDs over x**

$$d^4 \bar{\sigma} + d^4 \vec{\sigma} = \underbrace{2\Re e(T^{DVCS} \cdot T^{BH})}_{\downarrow} + \underbrace{|T^{DVCS}|^2}_{\text{Known}} + \underbrace{|T^{BH}|^2}_{\text{(fully calculable with nucleon FFs)}}$$

$$T^{DVCS} \propto \boxed{P \int_{-1}^{+1} \frac{GPD(x, \xi, t)}{x - \xi} dx} \pm i \boxed{\Pi GPD(x = \pm \xi, \xi, t)} + \dots$$

The **polarized cross-section difference** accesses the **imaginary** part of the **interference** and therefore **GPDs at  $x = \pm \xi$**

$$d^4 \bar{\sigma} - d^4 \vec{\sigma} = \boxed{2\Im m(T^{DVCS} \cdot T^{BH})}$$

# Deeply Virtual Compton Scattering

**At leading order (LO) and leading twist (LT) (twist-2):**

$$d^4 \bar{\sigma} - d^4 \bar{\sigma} = 2\Im(T^{DVCS} \cdot T^{BH})$$

$$d^4 \bar{\sigma} + d^4 \bar{\sigma} = 2\Re(T^{DVCS} \cdot T^{BH}) + |T^{DVCS}|^2 + |T^{BH}|^2$$

Known  
(fully calculable  
with nucleon FFs)

**Bilinear combination of Compton Form Factors CFFs**

$$C^{DVCS}(\mathcal{F}, \mathcal{F}^*) \propto 4(1-x_B) \mathcal{H} \mathcal{H}^* - f(x_B, Q^2, t)(\mathcal{H} \mathcal{E}^* + \mathcal{E} \mathcal{H}^*) + \dots$$

## Linear combination of CFFs

$$C^I(\mathcal{F}) = F_1(t)\mathcal{H} + \frac{x_B}{2-x_B}(F_1(t) + F_2(t))\tilde{\mathcal{H}} - \frac{t}{4M^2}F_2(t)\mathcal{E}$$

$$\left\{ \begin{array}{l} \text{Re}(\mathcal{H}) = \sum_q P \int_{-1}^1 dx \left( \frac{1}{x-\xi} \pm \frac{1}{x+\xi} \right) \mathcal{H}^q(x, \xi, t) \\ \Im m(\mathcal{H}) = -\pi \sum_q e_q^2 \left( \mathcal{H}^q(x=\xi, \xi, t) - \mathcal{H}^q(x=-\xi, \xi, t) \right) \end{array} \right. \quad \text{GPDs}$$

BMK : Belitsky et al.  
Phys.Rev.D82:074010,2010  
BMP : Braun et al.  
Phys.Rev.D89:074022,2014

 We can extract 8 GPDs observables at LO/LT:  $\Re e$  and  $\Im m \left( \mathcal{F} \in \{\mathcal{H}, \tilde{\mathcal{H}}, \mathcal{E}, \tilde{\mathcal{E}}\} \right)$

# Deeply Virtual Compton Scattering

---

Access to GPDs via **the unpolarized cross section :**

- Subtract the known contribution of BH

$$d^4 \overleftarrow{\sigma} + d^4 \overrightarrow{\sigma} = 2\Re e(T^{DVCS} \cdot T^{BH}) + |T^{DVCS}|^2 + |T^{BH}|^2$$

Known  
(fully calculable  
with nucleon FFs)

# Deeply Virtual Compton Scattering

Access to GPDs via **the unpolarized cross section :**

- Studying the  $\varphi$  and  $E_{beam}$  dependence of  $I$  and  $|T^{DVCS}|^2$  at fixed  $x_B$ ,  $Q^2$  and  $t$  allows to deduce some observables

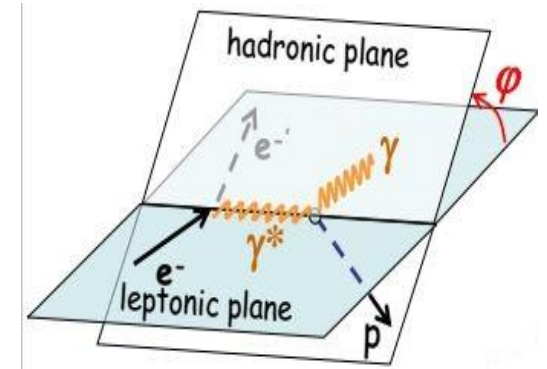
$$d^4 \overleftarrow{\sigma} + d^4 \overrightarrow{\sigma} = 2\Re e(T^{DVCS} \cdot T^{BH}) + |T^{DVCS}|^2 + |T^{BH}|^2$$

$|T^{DVCS}|^2 \propto \Gamma^{DVCS} E_{beam}^2 [c_0^{DVCS}(\mathcal{F}) + c_1^{DVCS}(\mathcal{F}) \cos \varphi + \dots]$

---

$2\Re e(T^{DVCS} \cdot T^{BH}) \propto \Gamma^I E_{beam}^3 [c_0^I(\mathcal{F}) + c_1^I(\mathcal{F}) \cos \varphi + c_2^I(\mathcal{F}) \cos 2\varphi + c_3^I(\mathcal{F}) \cos 3\varphi + \dots]$

$\mathcal{F} \in \{\mathcal{H}, \tilde{\mathcal{H}}, \mathcal{E}, \tilde{\mathcal{E}}\}$  : Compton Form Factors CFFs



# Motivation (DVCS off the neutron)

❖ DVCS off the **neutron** :  $F_1(t) \ll F_2(t)$

$$C^I(\mathcal{F}) = F_1(t)\mathcal{H} + \frac{x_B}{2-x_B}(F_1(t) + F_2(t))\tilde{\mathcal{H}} - \frac{t}{4M^2}F_2(t)\mathcal{E}$$

➤ Sensitive to **GPD E** (least constrained GPD) and which is important to access **quarks orbital momentum** via Ji's sum rule:

$$\frac{1}{2} \int_{-1}^{+1} dx x [H_q(x, \xi, t=0) + E_q(x, \xi, t=0)] = J^q = \frac{1}{2} \Delta \Sigma_q + L_q$$

❖ Neutron has different flavors from the proton => GPDs flavor separation:

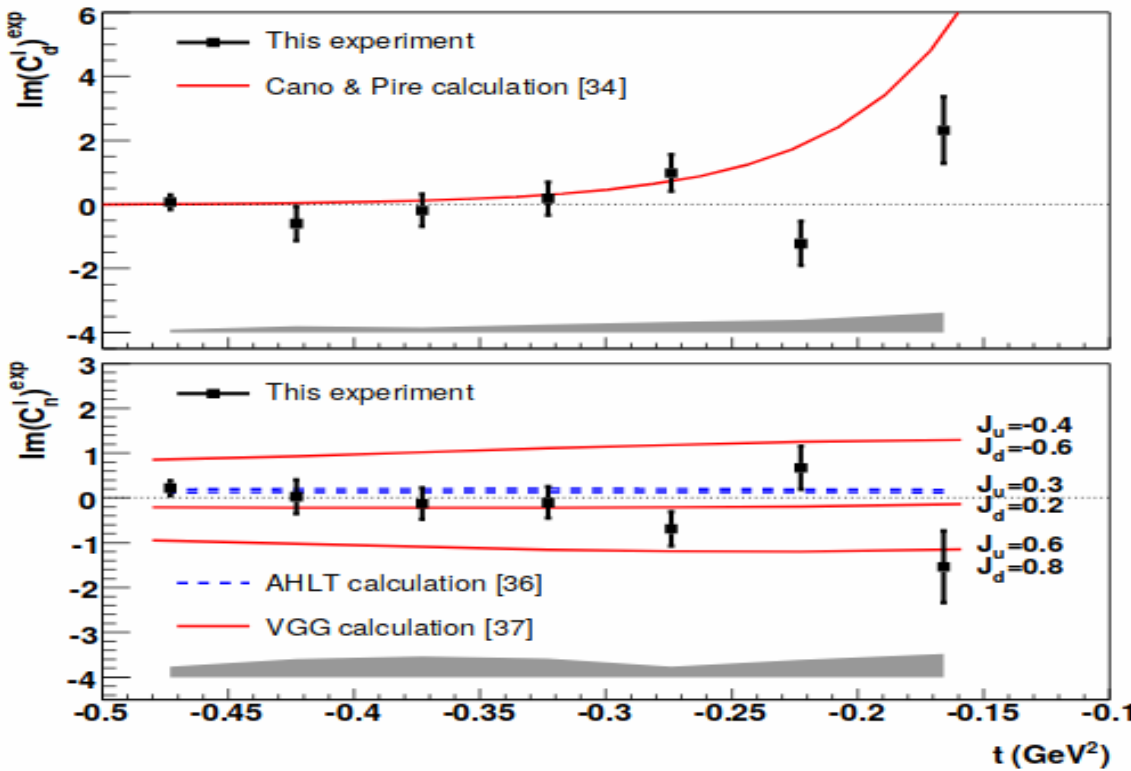
$$H^p(\xi, \xi, t) = \frac{4}{9} H^u(\xi, \xi, t) + \frac{1}{9} H^d(\xi, \xi, t) \quad H^n(\xi, \xi, t) = \frac{4}{9} H^d(\xi, \xi, t) + \frac{1}{9} H^u(\xi, \xi, t)$$

# DVCS off the neutron (Experiment E06-106)

E03-106: pioneer experiment of the DVCS off the neutron (2004):

Polarized cross section difference was determined at:  $Q^2=1.91 \text{ GeV}^2$ ;  $x_B=0.36$ ,  $E_{\text{beam}}=5.75 \text{ GeV}$

M. MAZOUZ *et al.*, Phys. Rev. Lett. 99:242501, 2007



Unpolarized cross section could not be extracted (huge systematic uncertainties)



Next experiment

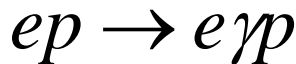
# Experimental setup

The **E08-025** (n-DVCS) experiment was performed at **JLab Hall A** in 2010

➤ Goal : Measure the **n-DVCS total cross-section**

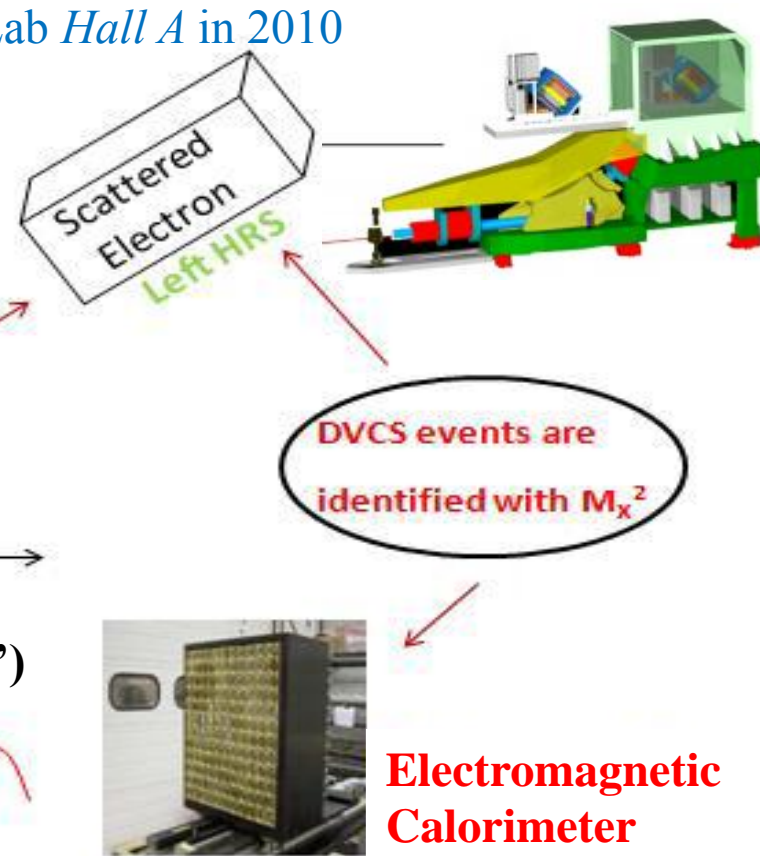
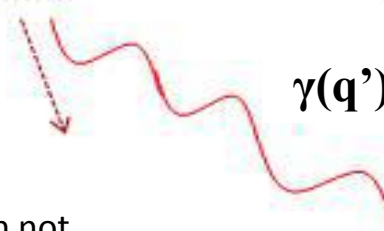
**Beam Energy = 4.45 GeV & 5.54 GeV**

$I_{beam} \approx 2-3 \mu\text{A}$  (80% polar.)



$P(p')$

Recoil  
nucleon not  
detected



❖ The data were taken at two kinematics (**Kin2high** and **Kin2low**):

✓  $Q^2 = 1.75 \text{ GeV}^2$

✓  $x_{Bj} = 0.36$

✓  $t \sim [-0.5, -0.1] \text{ GeV}^2$

✓ Maximal luminosity =  $3 \cdot 10^{37} \text{ cm}^{-2} \text{s}^{-1}$

- 13 X 16 PbF<sub>2</sub> blocs (density 7.77 g/cm<sup>3</sup>)
- block size : 3x3 cm<sup>2</sup> x 20 X<sub>0</sub>
- Each blok is conected to (PM + base)
- The detection Based on Čerenkov light detection

# Selection of the n-DVCS events

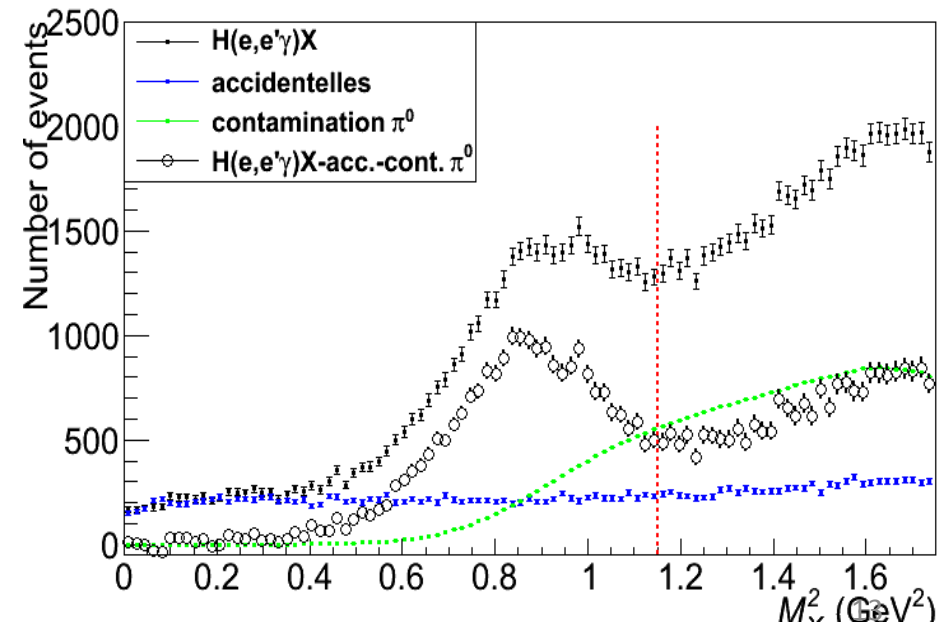
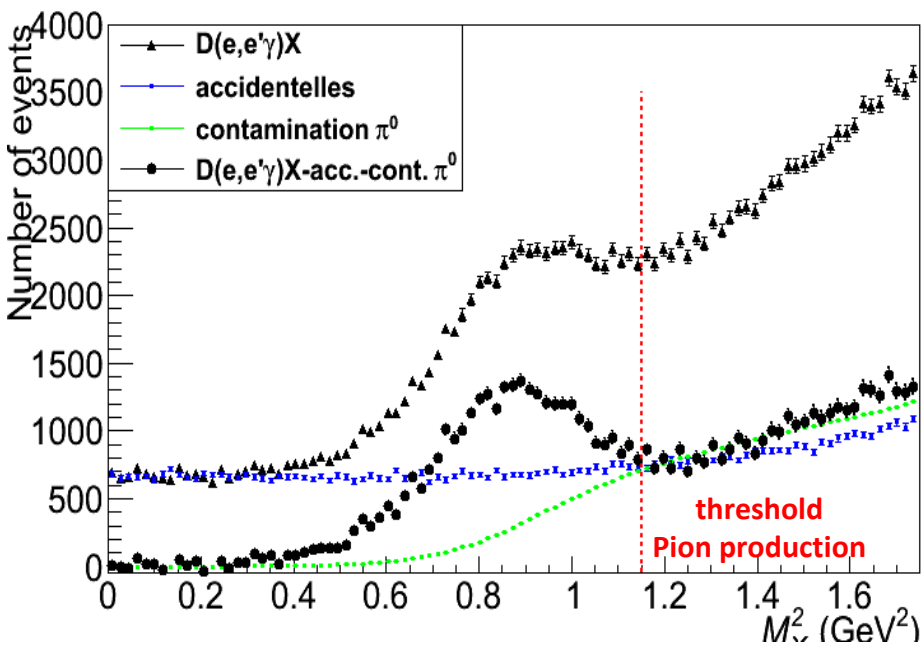
## Accidentals && $\pi^0$ contamination subtraction

The raw data: detect  $e'$  and  $\gamma$  in coincidence ( $eN \rightarrow e' \gamma X$ )

- 1 track in the HRS and 1 cluster in the calorimeter (energy  $> 1$  GeV)

- The detected photon may be in fortuitous coincidence with the scattered electron
- The photon detected in the calorimeter may come from the decay of  $\pi^0$  and resembles kinematically to a DVCS photon :  $eN \rightarrow e'\pi^0 X \rightarrow e' \gamma_1 \gamma_2 X$

$$\text{Spectrum : } M_X^2 = (e + N - e' - \gamma)^2$$



# Selection of the n-DVCS events

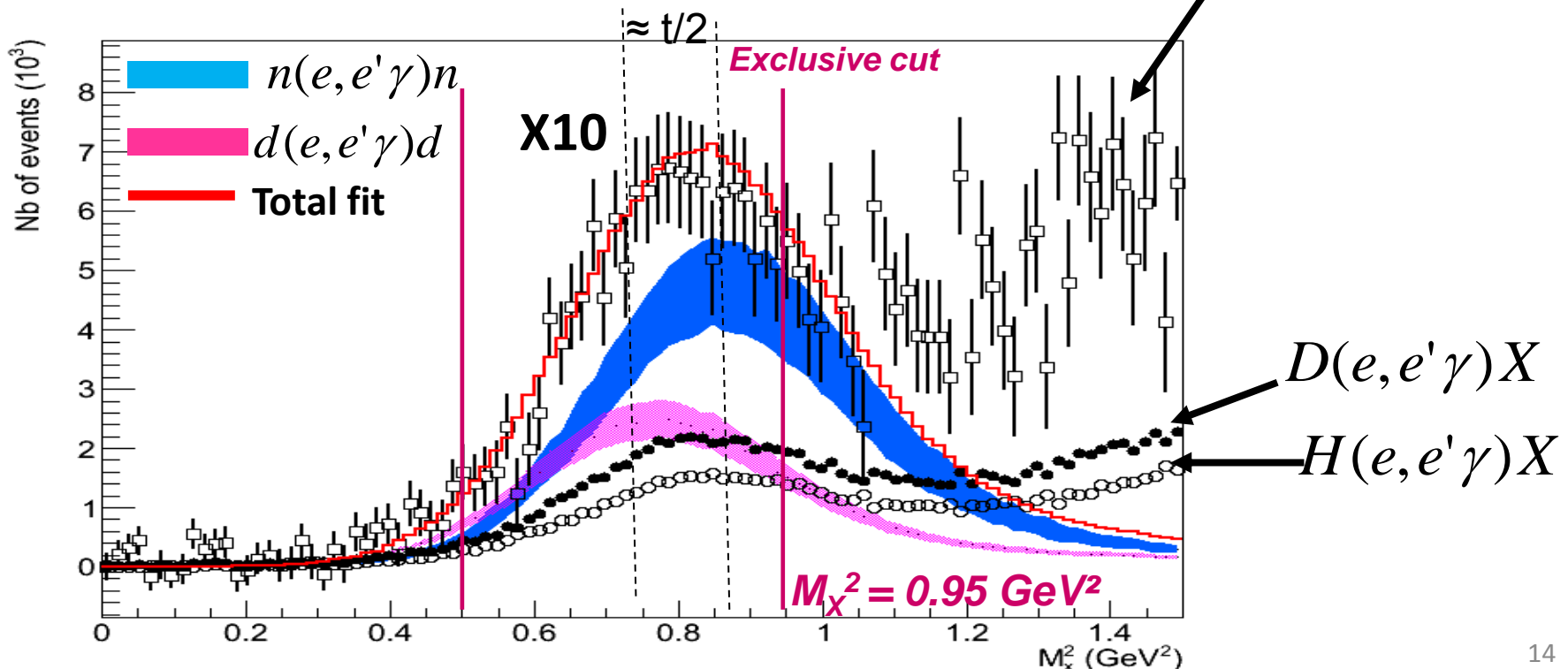
After

- subtracting the accidentals,
- subtracting single photons coming from  $\pi^0$  decay ( $\pi^0$  contamination),
- adding Fermi momentum to H2 data,
- normalizing H2 and D2 data to the same luminosity,

We obtain the difference

$$D(e, e'\gamma)X - H(e, e'\gamma)X \\ = n(e, e'\gamma)n + d(e, e'\gamma)d + \dots$$

$$D(e, e'\gamma)pn = p(e, e'\gamma)p + n(e, e'\gamma)n + d(e, e'\gamma)d$$



# Adjusting the simulation to the experimental data

Experimental data

+

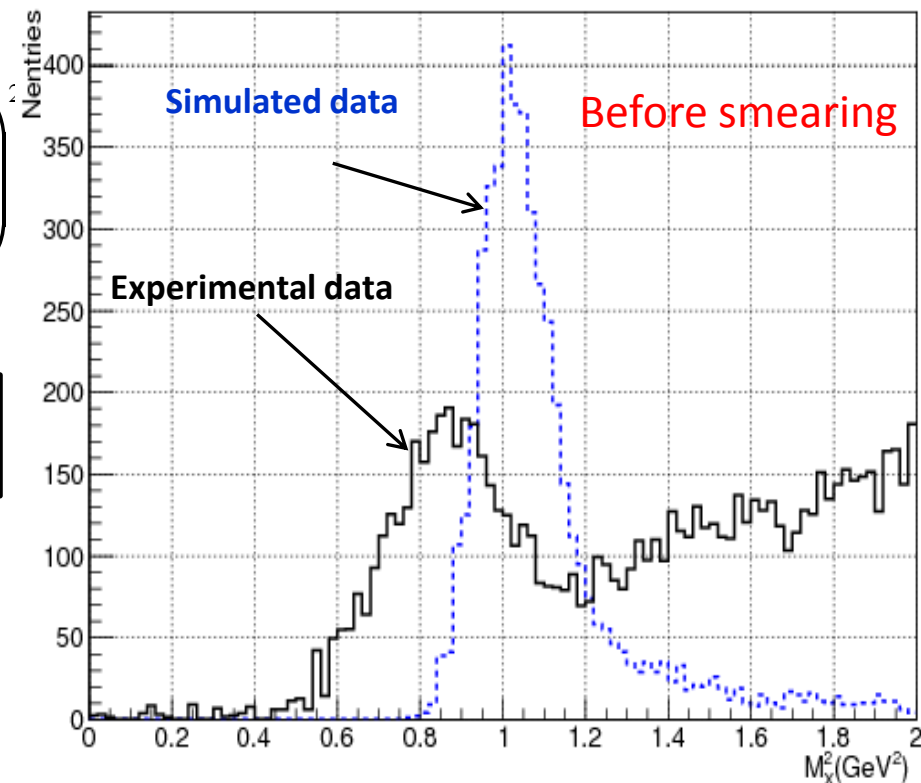
simulated data:

- 1- have the same cuts applied to the experimental data
- 2- have the same resolution and the same calibration as experimental data
- 3- takes into account the radiative corrections

Adjustment :

$$\chi^2 = \sum_{e=0}^{Nbin} \left( \frac{N_e^{sim} - N_e^{exp}}{\Delta\sigma_e^{exp}} \right)^2$$

Cross Section  $\sigma^{exp}$



# Adjusting the simulation to the experimental data

Experimental data

+

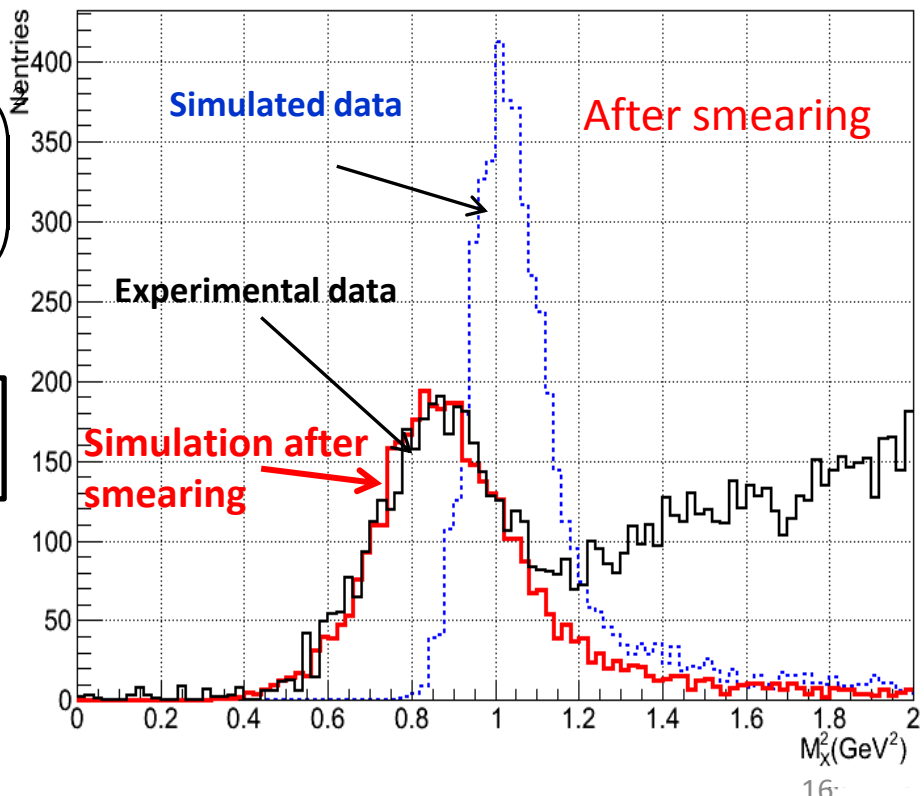
simulated data:

- 1- have the same cuts applied to the experimental data
- 2- have the same resolution and the same calibration as experimental data
- 3- takes into account the radiative corrections

Adjustment :

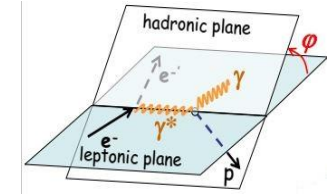
$$\chi^2 = \sum_{e=0}^{Nbin} \left( \frac{N_e^{sim} - N_e^{exp}}{\Delta\sigma_e^{exp}} \right)^2$$

Cross Section  $\sigma^{exp}$



# n-DVCS cross section (+d-DVCS)

Binning:  $12 \times 2 \times 5 \times 30$  bins in  $\phi$ ,  $E$ ,  $t$  and  $M_X^2$



- Dependence in  $\phi \rightarrow$  Separate the different neutron LO/LT CFFs observables  $X_{in}$  (neutron) (or  $X_{id}$  (coherent deuton))
- Binning in  $M_X^2 \rightarrow$  Separate  $n(e,e'\gamma)n$  and  $d(e,e'\gamma)d$  contributions  

$$M_X^2 d \approx M_X^2 n + t/2$$

The unpolarized (nDVCS + dDVCS) total cross section (simplified expression) :

$$\frac{d^4\sigma_{(nDVCS + dDVCS)}}{dQ^2 dx_B dt d\phi} = BH_n + BH_d + \sum_i \underbrace{\Gamma_{in}(Q^2, x_B, t, \phi)}_{\text{Kinematical factor}} \boxed{X_{in}} + \sum_i \underbrace{\Gamma_{id}(Q^2, x_B, t, \phi)}_{(DVCS^2+I) \text{ Coherent deuteron Contribution}} \boxed{X_{id}}$$

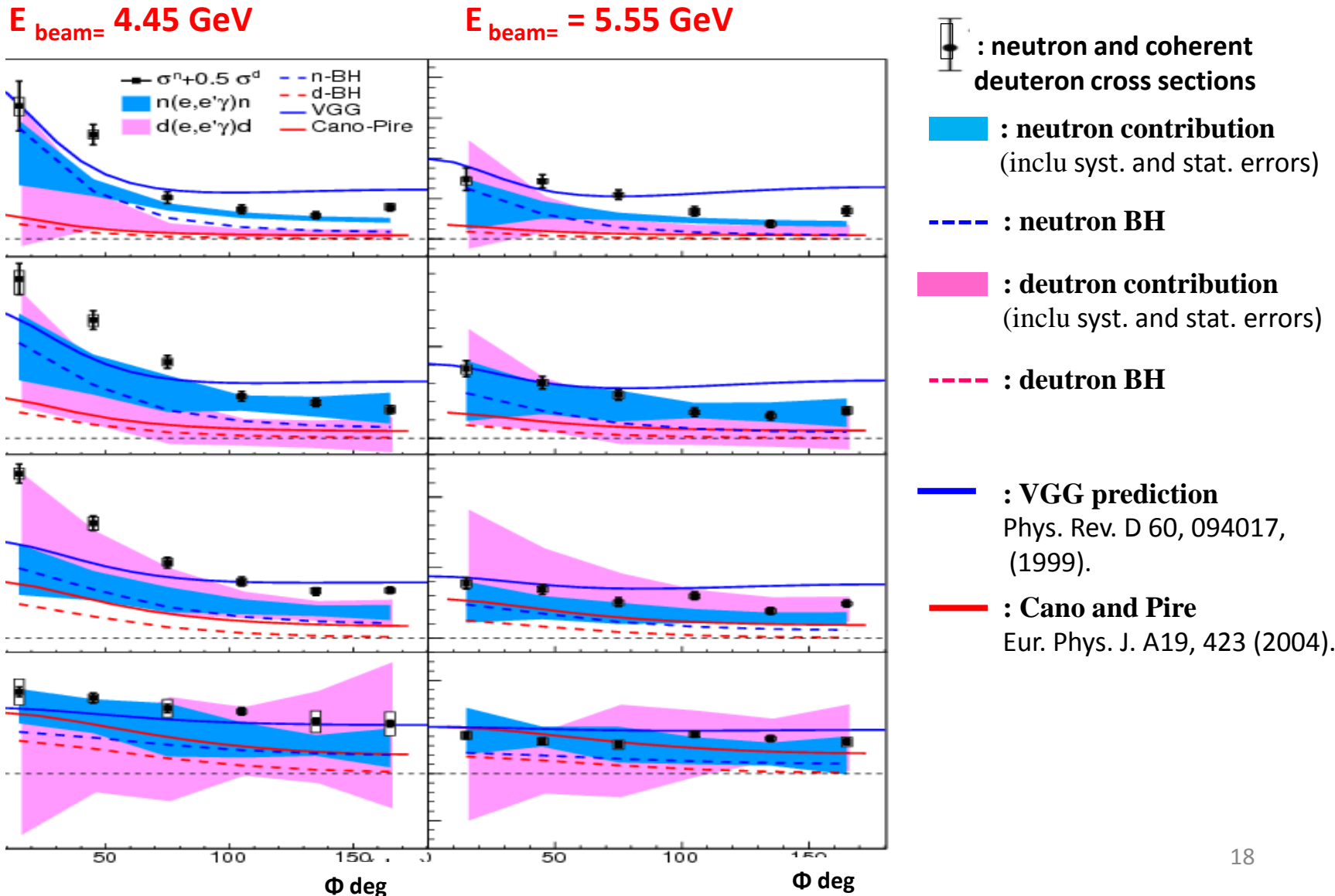
Annotations:

- $BH_{\text{neutron contribution}}$  points to the first term  $BH_n$ .
- $BH_{\text{coherent deuteron contribution}}$  points to the second term  $BH_d$ .
- $(DVCS^2+I)$  points to the third term  $\sum_i \Gamma_{in}(Q^2, x_B, t, \phi) X_{in}$ .
- $(DVCS^2+I)$  points to the fourth term  $\sum_i \Gamma_{id}(Q^2, x_B, t, \phi) X_{id}$ .

The observables we want to extract:  
the linear combinations of CFFs  
which contain GPDs

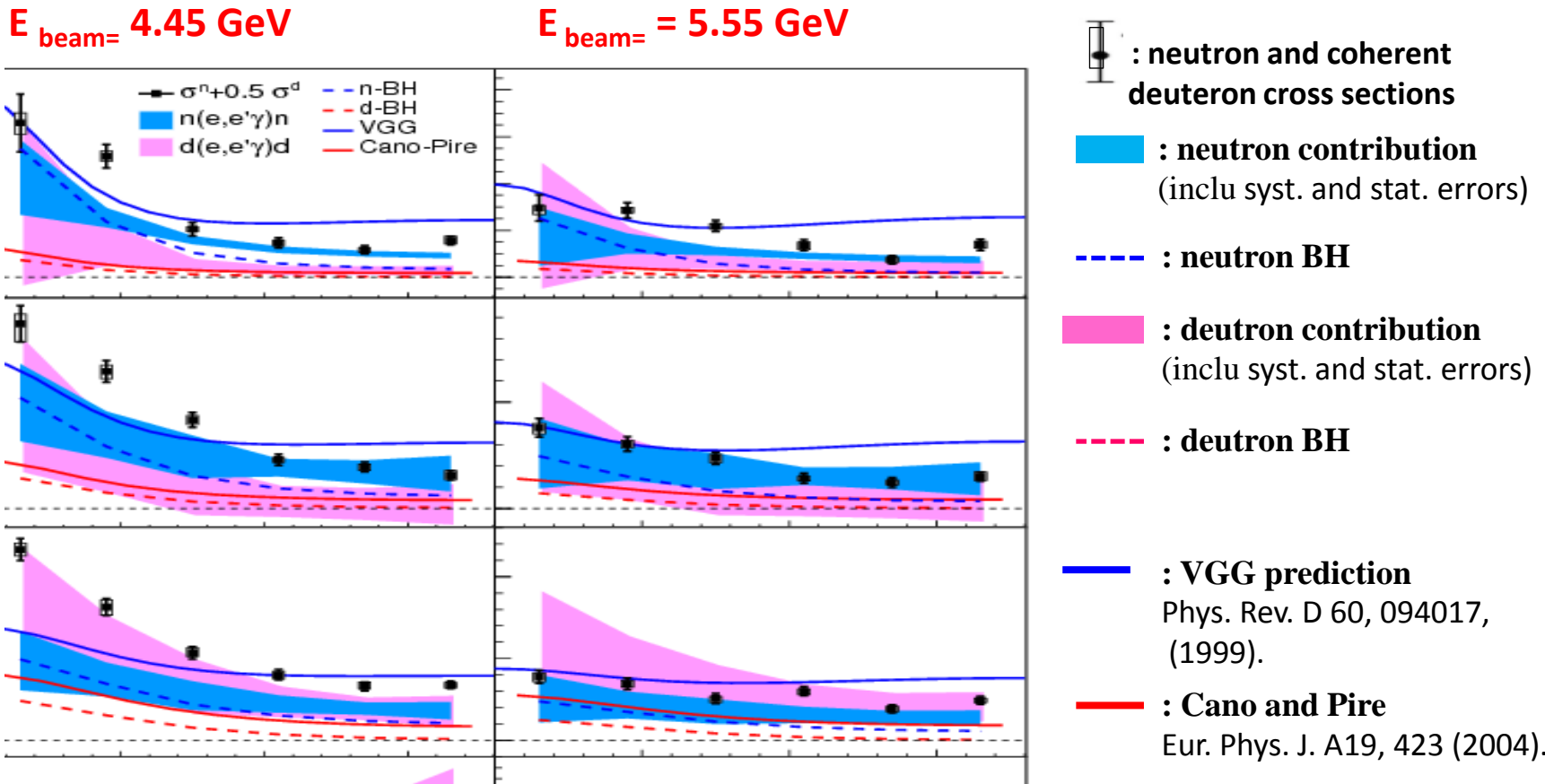
# n-DVCS cross section (+d-DVCS)

Unpolarized cross section as a function of  $\phi$ , E and t bins :



# n-DVCS cross section (+d-DVCS)

Unpolarized cross section as a function of  $\phi$ , E and t bins :



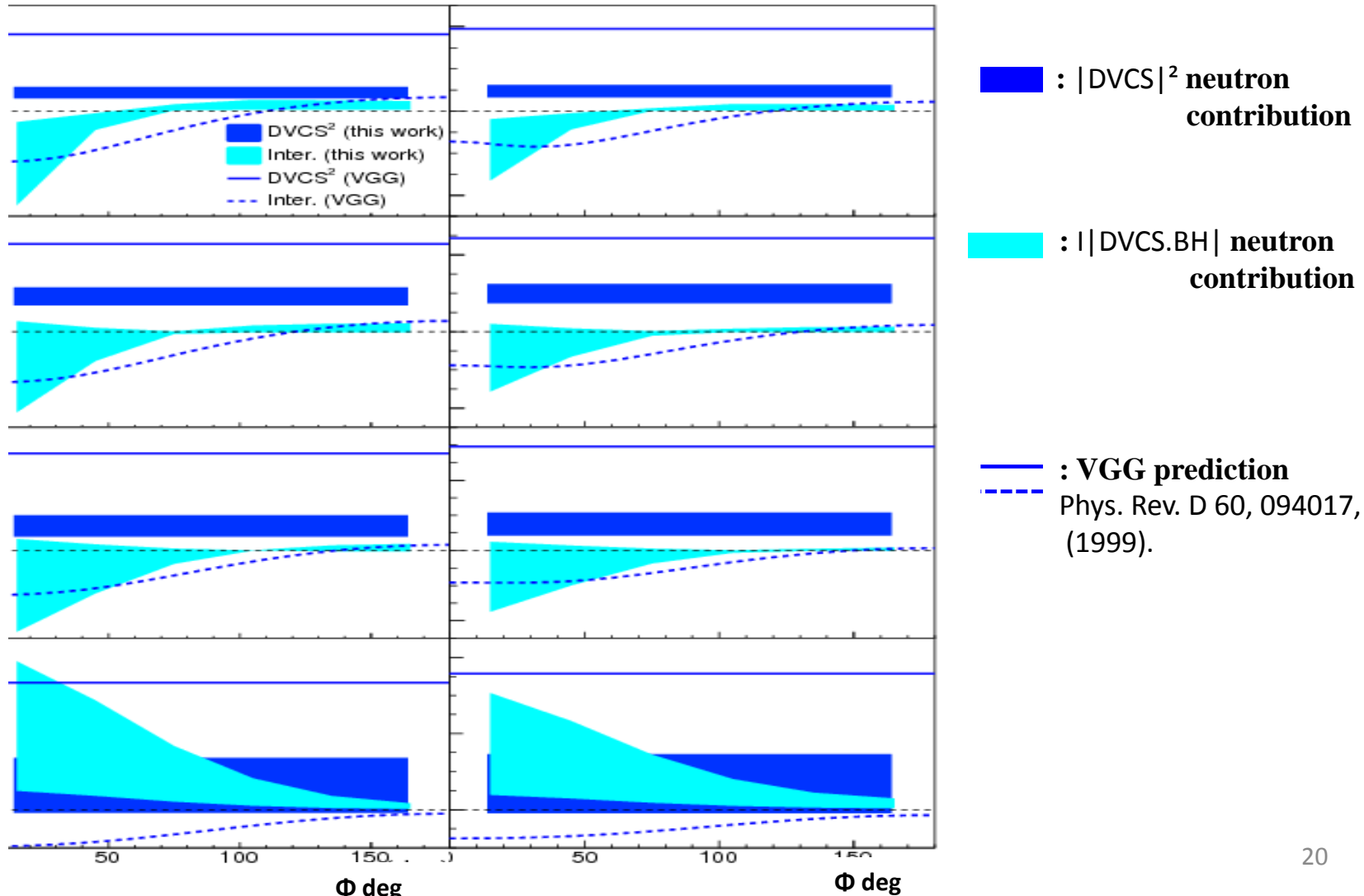
- First experimental determination of the unpolarized cross section
- the first experimental evidence of a **positive n-DVCS signal**

# n-DVCS cross section (+d-DVCS)

Simultaneous fit of two  $E_{\text{beam}}$  → Separate  $|\text{DVCS}|^2$  and  $I|\text{DVCS.BH}|$  contributions

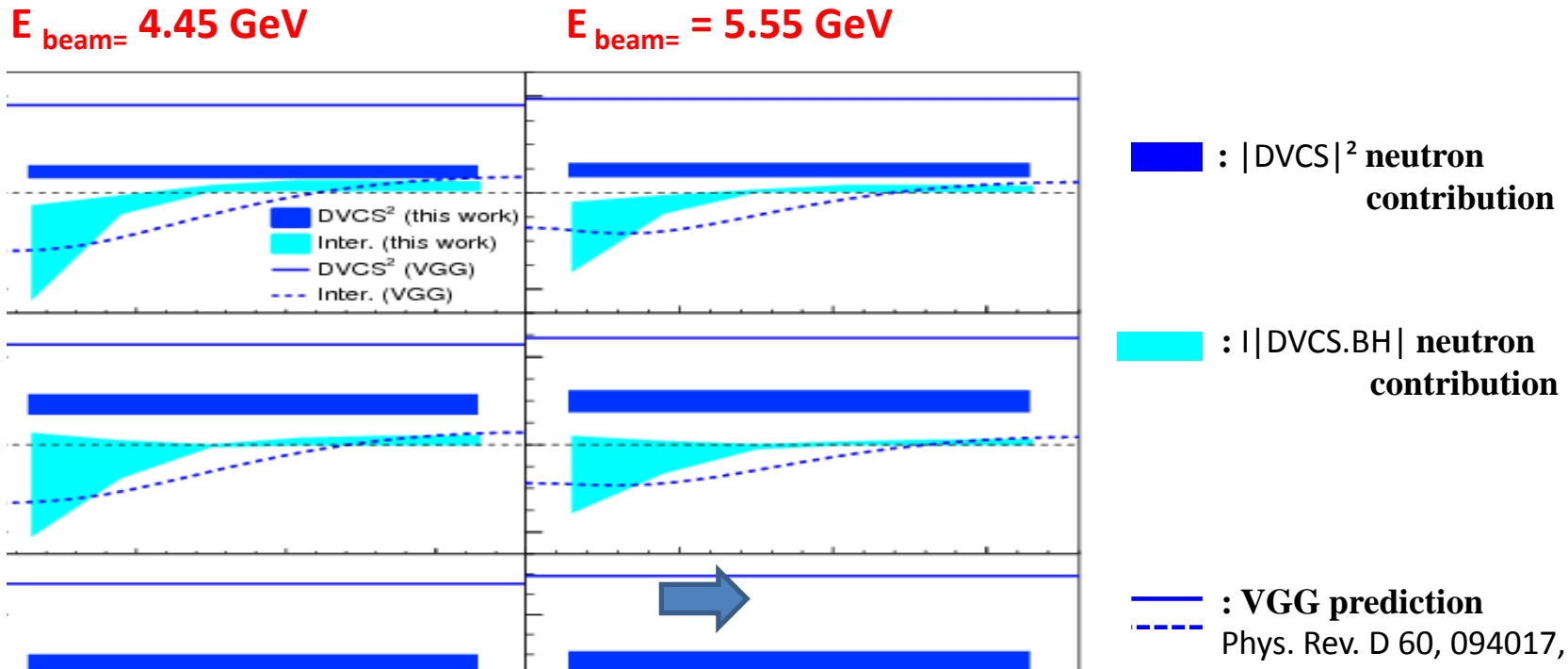
$E_{\text{beam}} = 4.45 \text{ GeV}$

$E_{\text{beam}} = 5.55 \text{ GeV}$



# n-DVCS cross section (+d-DVCS)

$|DVCS|^2$  and  $|DVCS.BH|$  contributions off the neutron as a function of  $\phi$ , E and t bins :



- The interference term is compatible with zero within error bars ( In agreement with E03-106 experiment 2004, M. MAZOUZ *et al.*, Phys. Rev. Lett. 99:242501, 2007 )
- The DVCS<sup>2</sup> has a significant contribution to the cross section (in agreement with proton results at the same kinematics : M. Defurne *et al.*, Nature Commun. 8, 1408, 2017)

# Conclusion

---

- First measurements of the unpolarized cross section of the photon electroproduction off a deuterium target
  - Rosenbluth separation of the DVCS<sup>2</sup> and the interference terms for the neutron and the coherent deuteron
  - Neutron results: significant deviation of the cross section from the n-BH :  
a non-zero n-DVCS signal
  - Deuteron results: compatible with d-BH and theoretical expectations
- 
- A flavor decomposition of the CFFs can be performed by combining proton and neutron data
  - The neutron results are sensitive to GPD E and can be exploited to constraint the quark angular momentum

**Thank you for your attention**

# **BACK-UP**

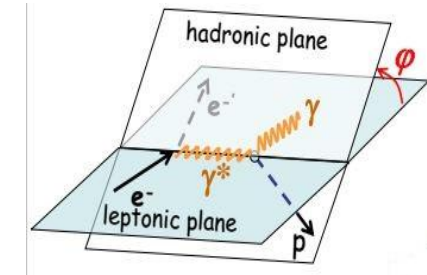
# Extraction of the cross section

According to the formalism of Muller Belitsky and the differential cross section is:

$$d^4\sigma = |T^{DVCS}|^2 + 2 T^{BH} \Re e(T^{DVCS}) + |T^{BH}|^2$$

$$|T^{DVCS}|^2 \propto \Gamma_0^{DVCS} C_0^{DVCS} + \Gamma_1^{DVCS} C_1^{DVCS} \cos(\varphi)$$

Terme connu



$$C_0^{DVCS} \propto \Gamma^{DVCS} C^{DVCS}(\mathcal{F}, \mathcal{F}^*) + \Gamma^{DVCS} C^{DVCS}(\mathcal{F}_{eff}, \mathcal{F}_{eff}^*)$$

1

$$I \propto \Gamma_0^I C_0^I + \Gamma_1^I C_1^I \cos(\varphi) + \Gamma_2^I C_2^I \cos(2\varphi) + \Gamma_3^I C_3^I \cos(3\varphi)$$

$$C_n^I = \Gamma^I \Re e C_{++}^I(n | \mathcal{F}) + \Gamma^I \Re e C_{0+}^I(n | \mathcal{F}_{eff}) + \Gamma^I \Re e C_{-+}^I(n | \mathcal{F}_\tau)$$

$$\Re e C_{++}^I(n | \mathcal{F}) = \Re e C^I(\mathcal{F}) + \frac{C^v(n)}{C_{++}(n)} \Re e C^{I,v}(\mathcal{F}) + \dots$$

2

$$\Re e C_{0+}^I(n | \mathcal{F}_{eff}) = [\dots] \Re e C^I(\mathcal{F}_{eff}) + \frac{C^v(n)}{C_{0+}(n)} \Re e C^{I,v}(\mathcal{F}_{eff}) + \dots$$

3

# Electromagnetic Calorimeter

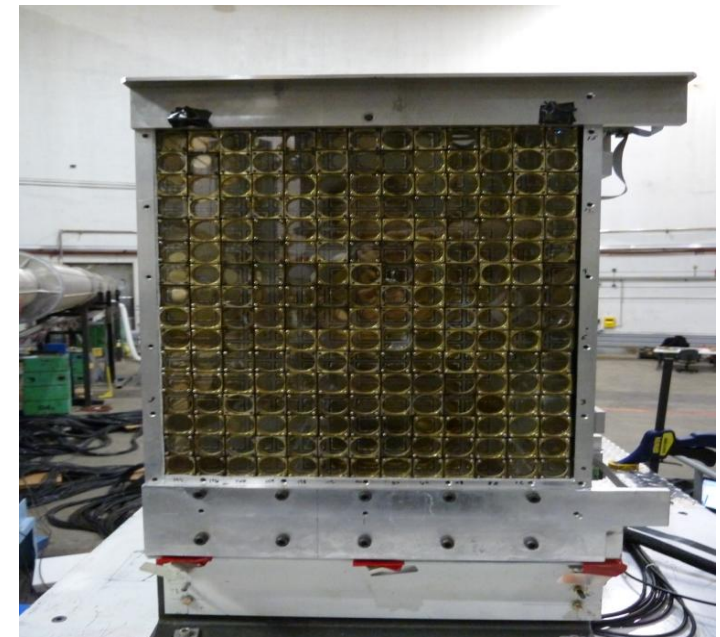
## Electromagnetic Calorimeter

- 13x16 PbF<sub>2</sub> blocks (Čerenkov light detection)
- Block size: 3x3 cm<sup>2</sup> x 20 X<sub>0</sub>
- short radiation length :  
-> X<sub>0</sub>=(1/20) crystal length
- Molière radius=2.2 cm
- > electromagnetic shower is contained in 9 adjacent blocks
- Each block is connected to (PMT + base + ARS)

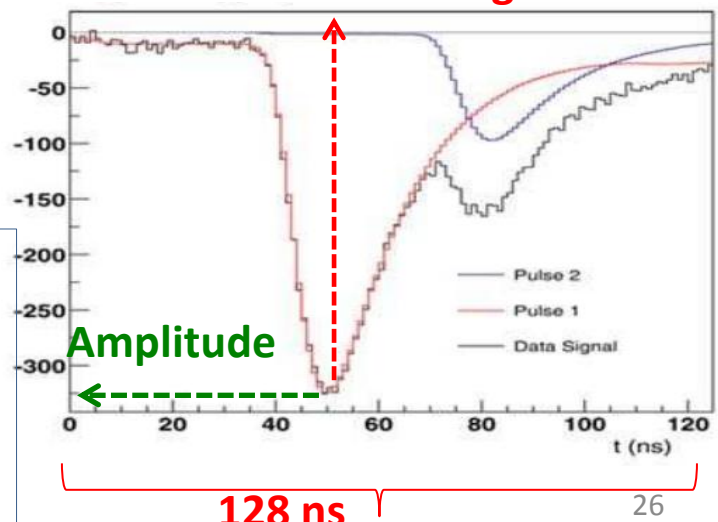
- ✓ recording the input signal on 128 ns (ARS) as in a digital oscilloscope in order to solve the pile up signals.
- ✓ Digitization and recording of all calorimeter channels for each electron detected in HRS (trigger)
- ✓ The energy deposit determination is based on a wave form analysis of the ARS signals.

## blackening blocks under the effects of radiation:

- the gains of the blocks decreases
- Calibrate the response of the electromagnetic calorimeter

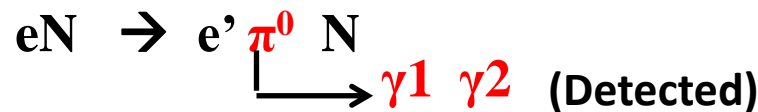


arrival times signal



# Calorimeter energy calibration

## Calibration method



The **calibration method** is based on the **comparison** between the **measured energy** of a detected  $\pi^0$  from  $H(e,e'\pi^0)p$  events and its expected **energy calculated** with its scattering angle:

$$\cos(\theta_{\gamma^*\pi^0}) = \frac{\vec{q}_{\gamma^*} \cdot \vec{q}_{\pi^0}}{\|\vec{q}_{\gamma^*}\| \cdot \|\vec{q}_{\pi^0}\|}$$

$$\chi^2 = \sum_{j=1}^N (E_\pi^j - \sum_{i=0}^{207} C_i E_i^j)^2$$

??

After the minimization we get the coefficients

$$\frac{\partial \chi^2}{\partial C_i} = 0 \Rightarrow [C_i] = [M]^{-1} [B]$$

The momentum of  $\pi^0$  reconstructed using  $\vec{q}_{\gamma_1}$  et  $\vec{q}_{\gamma_2}$  several iterations to get the final coefficients for each block i

$$\Rightarrow C_i^{final} = C_i^{iter1} \times C_i^{iter2} \times \dots \times C_i^{iter7}$$

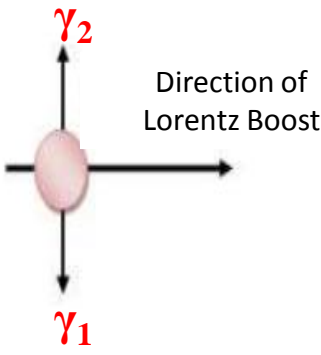
# Selection of the n-DVCS events

## 2- $\pi^0$ contamination subtraction

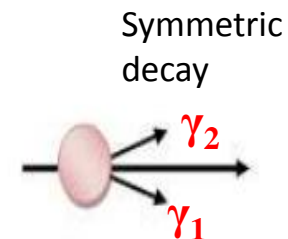
→ The photon detected in the calorimeter may come from the decay of  $\pi^0$  and resembles kinematically to a DVCS photon :  $eN \rightarrow e'\pi^0 X \rightarrow e' \gamma_1 \gamma_2 X$

$\pi^0$  decay in  $\gamma_1 \gamma_2$

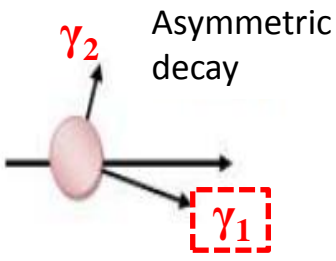
CM frame



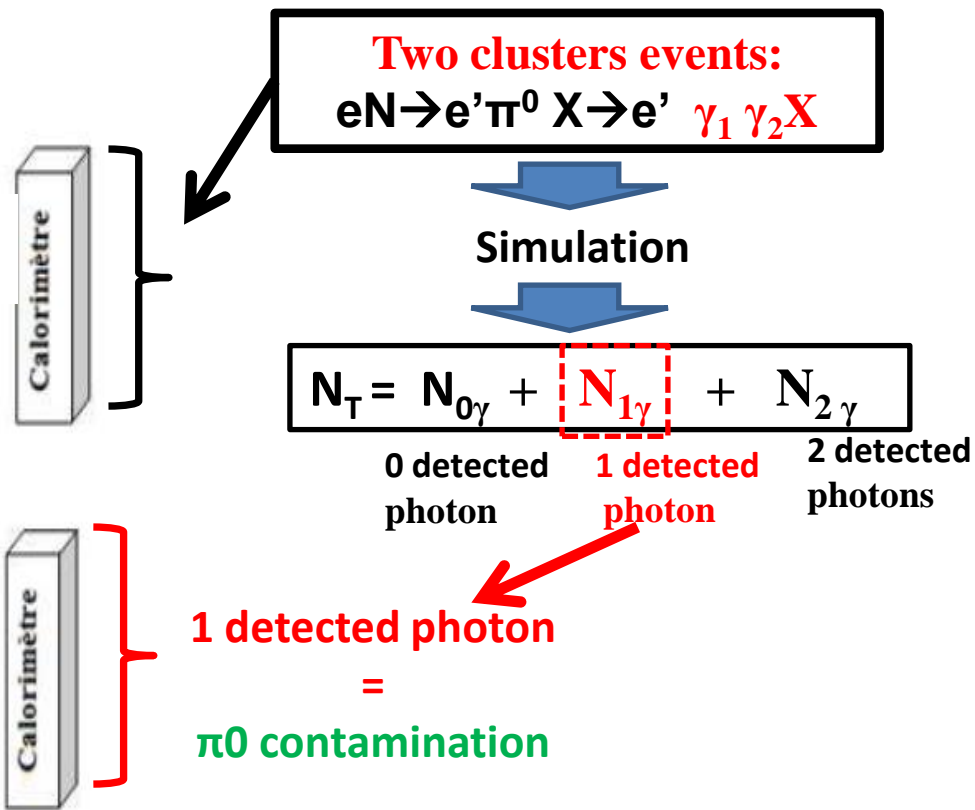
Laboratory frame



Symmetric decay



Asymmetric decay



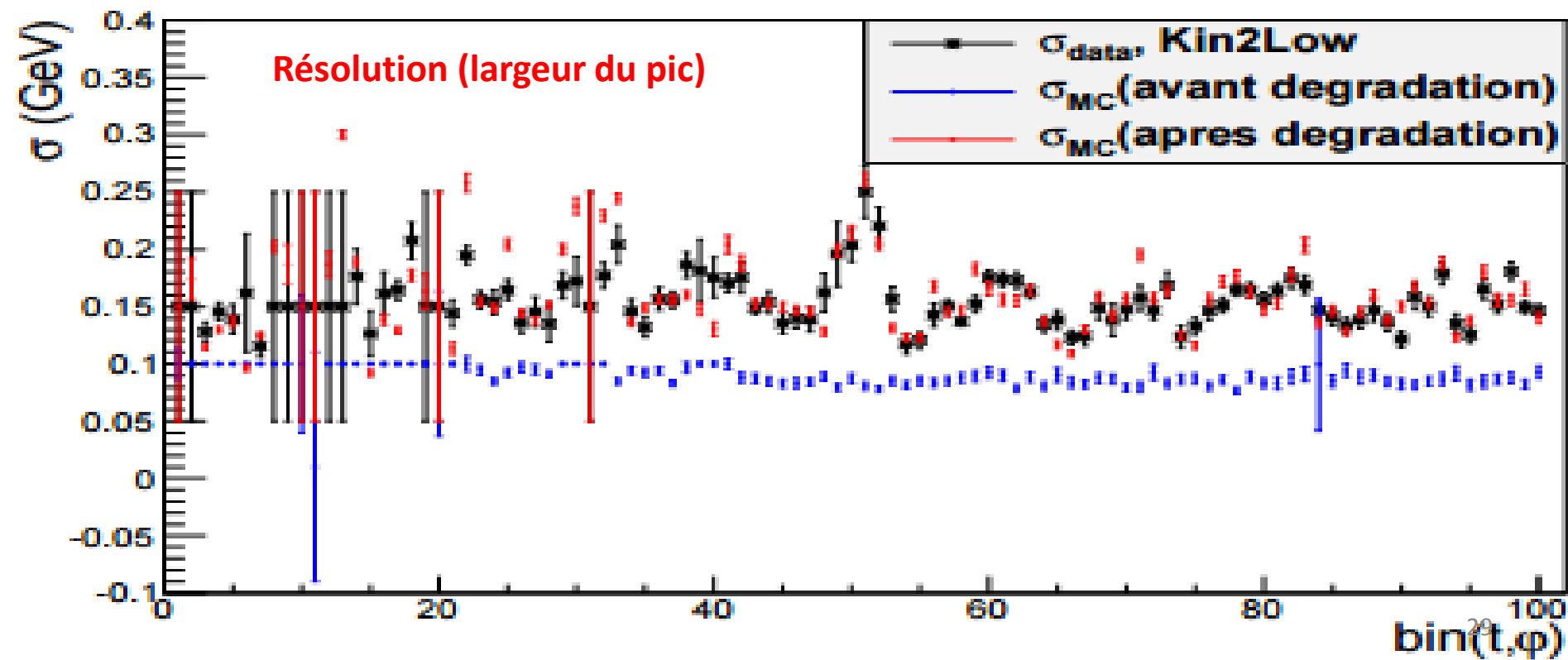
- We applied a cut on the blocks of the edges and on the corner of the calorimeter to better estimate the  $\pi^0$  contamination (Efficiency = 100% +/- 1)

# Smearing of the simulation data

## Smearing Result

For 5 in t and 20 in  $\phi$

- Good agreement between the resolution of the data and the simulation for each bin ( $t$  and  $\phi$ )
- Good agreement between the calibration of the data and the simulation for each bin ( $t$  and  $\phi$ )
- The first 20 bins are rejected (blocks on board of the calorimeter)
- The coefficients of the smearing determined with LH2\_data and the p\_DVCS simulation are then applied to d\_DVCS and n\_DVCS simulation.



# Smearing of the simulation data

## Smearing Result

For 5 in t and 20 in  $\phi$

- Good agreement between the resolution of the data and the simulation for each bin ( $t$  and  $\phi$ )
- Good agreement between the calibration of the data and the simulation for each bin ( $t$  and  $\phi$ )
- The first 20 bins are rejected (blocks on board of the calorimeter)
- **The coefficients of the smearing determined with LH2\_data and the p\_DVCS simulation are then applied to d\_DVCS and n\_DVCS simulation.**

